Rab6 is required for the exocytosis of cortical granules and the recruitment of separase to the granules during the oocyte-to-embryo transition in *Caenorhabditis elegans*

Kenji Kimura and Akatsuki Kimura*

Cell Architecture Laboratory, Structural Biology Center, National Institute of Genetics, Mishima 411-8540, Japan

*Author for correspondence (akkimura@nig.ac.jp)

Accepted 24 August 2012
Journal of Cell Science 125, 5897–5905

doi: 10.1242/jcs.116400

Summary

Remodeling of the embryo surface after fertilization is mediated by the exocytosis of cortical granules derived from the Golgi complex. This process is essential for oocyte-to-embryo transition in many species. However, how the fertilization signal reaches the cortical granules for their timely exocytosis is largely unknown. In *Caenorhabditis elegans*, the recruitment of separase, a downstream effector of the fertilization signal, to the cortical granules is essential for exocytosis because separase is required for membrane fusion. However, the molecule that recruits separase to the cortical granules remains unidentified. In this study, we found that Rab6, a Golgi-associated GTPase, is essential to recruit separase to the cortical granules in *C. elegans* embryos. Knockdown of the *rab-6.1* gene, a Rab6 homolog in *C. elegans*, resulted in failure of the membrane fusion step of cortical granule exocytosis. Using a transgenic strain that expresses GFP-fused RAB-6.1, we found that RAB-6.1 temporarily co-localized with separase on the cortical granules for a few minutes and then was dispersed in the cytoplasm concomitantly with membrane fusion. We found that RAB-6.1, as well as cyclin-dependent kinase (CDK)-1 and anaphase promoting complex/cyclosome (APC/C), was required to recruit separase to the cortical granules. RAB-6.1 was not required for the chromosome segregation process, unlike CDK-1, APC/C and SEP-1. The results indicate that RAB-6.1 is required specifically for the membrane fusion step of exocytosis and for the recruitment of separase to the granules. Thus, RAB-6.1 is an important molecule for the timely exocytosis of the cortical granules during oocyte-to-embryo transition.

Key words: *Caenorhabditis elegans*, Cortical granule exocytosis, Rab GTPase, Separase

Introduction

After fertilization, oocytes undergo a series of dramatic changes collectively called oocyte-to-embryo transition, which are essential for the onset of embryogenesis in many species (Ferrell, 1999; Wessel et al., 2001; Runft et al., 2002; Pellettieri et al., 2003; Horner and Wolfner, 2008). These changes include an increase in the intracellular calcium concentration (Ca^{2+}), cytoskeletal rearrangement, the resumption of the cell cycle, and the exocytosis of secretory vesicles called 'cortical granules' (Ferrell, 1999; Wessel et al., 2001; Runft et al., 2002; Horner and Wolfner, 2008). Cortical granules are derived from the Golgi complex and contain extracellular matrix components such as proteases and glycoproteins (Wessel et al., 2001). Because of cortical granule exocytosis, the embryo surface is reorganized to protect embryos from polyspermy and osmotic and mechanical stress and to allow molecules involved in embryo functions such as cytokinesis to localize on the embryo surface (Wessel et al., 2001; Mizuguchi et al., 2003; Olson et al., 2006).

Cortical granule exocytosis occurs within seconds after fertilization in sea urchins, starfish, and frogs (Wessel et al., 2001). The increased Ca^{2+} concentration upon fertilization affects the sub-processes of cortical granule exocytosis, such as the translocation of cortical granules to near the plasma membrane in mice (Kline and Kline, 1992; Matson et al., 2006) and soluble *N*-ethylmaleimide sensitive factor attachment protein receptor (SNARE)-dependent membrane fusion in sea urchins (Conner et al., 1997; Conner and Wessel, 2001). It has been proposed that in the latter sub-process, the Ca^{2+}-binding protein synaptotagmin promotes SNARE-dependent membrane fusion in response to Ca^{2+} (Leguia et al., 2006). However, cortical granule exocytosis does not always occur just after fertilization and the corresponding increase in Ca^{2+} levels, suggesting that Ca^{2+} is not the sole and direct trigger of the exocytosis. For example, in mice and *Caenorhabditis elegans*, cortical granule exocytosis occurs more than 5 min after fertilization (Fukuda and Chang, 1978; Sato et al., 2008), whereas the first Ca^{2+} increase occurs within 3 min after fertilization (Lawrence et al., 1997; Samuel et al., 2001).

C. elegans is a well-studied model for the oocyte-to-embryo transition and the subsequent cortical granule exocytosis (Marcello and Singson, 2010). In *C. elegans*, the timing of cortical granule exocytosis seems to be under the control of cell cycle regulators. In proximal oocytes, the cell cycle is arrested in meiotic prophase I, and cortical granules are located near the plasma membrane, but they are not secreted. Oocytes mature and proceed to metaphase I in response to a diffusive signal from the

spermatheca (McCarter et al., 1999; Kosinski et al., 2005). The cyclin-dependent kinase CDK-1 is required for the cell cycle progression (Boxem et al., 1999). After fertilization, the anaphase-promoting complex/cyclosome (APC/C) is activated to induce meiotic anaphase I, which is when cortical granule exocytosis occurs (Sato et al., 2006; Bembenek et al., 2007) (supplementary material Fig. S1). CDK-1 and the subunits of APC/C as well as the downstream effector of APC/C, separase, are required for cortical granule exocytosis in *C. elegans* (Sato et al., 2006; Bembenek et al., 2007). Generally, separase is activated at the metaphase-to-anaphase transition by the degradation of its binding partner securin by APC/C (Nasmyth, 2002). Interestingly, the *C. elegans* ortholog of separase, SEP-1 (Siomos et al., 2001), translocates to cortical granules just before exocytosis (Bembenek et al., 2007). In addition, SEP-1 is required for the fusion of secretory vesicles into the plasma membrane during cytokinesis (Bembenek et al., 2010). These results collectively indicate that the timing of cortical granule exocytosis is regulated by cell cycle regulators (i.e. CDK-1, APC/C, and SEP-1). Further, the localization of SEP-1 on cortical granules is likely critical for exocytosis, because *sep-1* alleles defective for cortical granule exocytosis are defective for SEP-1 localization on cortical granules, and a suppressor for the exocytosis defect also rescues the SEP-1 localization (Richie et al., 2011). However, the molecule that recruits separase to cortical granules remains unidentified.

Rab GTPases are important regulators of exocytosis in general, as they regulate budding, motility, tethering, and fusion of intracellular vesicles (Stenmark, 2009). During cortical granule exocytosis in *C. elegans*, RAB-11.1 (a Rab11 GTPase homolog) contributes to the targeting of cortical granules to the plasma membrane in oocytes before fertilization (Sato et al., 2008). However, the Rab GTPase involved in the fusion process during oocyte-to-embryo transition has not been identified.

Rab6 is known to play a key role in the membrane traffic around the Golgi complex. In mammalian cells, Rab6 cooperates with various effector proteins including motor proteins to regulate the fission of transport vesicles from the Golgi and the translocation of Golgi-derived vesicles along microtubules (Echard et al., 1998; Matanis et al., 2002; Grigoriev et al., 2007; Miserey-Lenkei et al., 2010; Grigoriev et al., 2011). In *Drosophila* oocytes, Rab6 helps establish cell polarity (Januschke et al., 2007). However, its role in cortical granule exocytosis has not been analyzed yet. In this study, we investigated the role of Rab6 in cortical granule exocytosis in *C. elegans*. We discovered a novel function of Rab6: the recruitment of separase on cortical granules for exocytosis during the oocyte-to-embryo transition.

Results

RAB-6.1 and RAB-6.2 localize to Golgi-derived granules in oocytes

The *C. elegans* genome has 2 Rab6 homologs, namely, *rab-6.1* and *rab-6.2*. We first examined whether RAB-6.1 and RAB-6.2 localize to the Golgi complex. We found that RAB-6.1 (tagged with the red fluorescence protein mCherry; mCherry::RAB-6.1) and RAB-6.2 [tagged with green fluorescence protein (GFP); GFP::RAB-6.2] co-localized to vesicular structures throughout the oocyte cytoplasm (Fig. 1A). The vesicles were adjacent to the Golgi marker ManS [tagged with yellow fluorescence protein (YFP); ManS::YFP] (Fig. 1B), suggesting that RAB-6.1/RAB-6.2 vesicles are derived from the Golgi complex. We also confirmed that the mCherry::RAB-6.1 construct can rescue the phenotype resulting from a *rab-6.1*-deletion mutation (supplementary material Fig. S2).

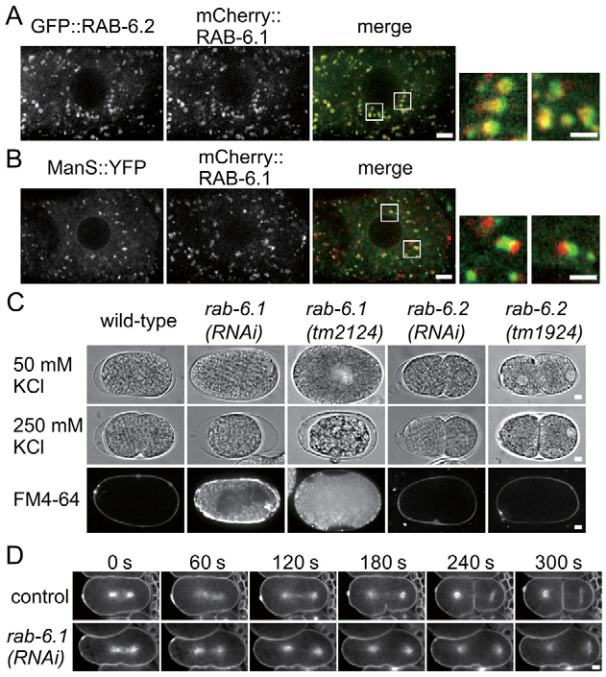

Fig. 1. RAB-6.1 is involved in cortical granule exocytosis. (**A**,**B**) Confocal fluorescence images of the most proximal oocyte expressing GFP::RAB-6.2 and mCherry::RAB-6.1 (A) and ManS::YFP and mCherry::RAB-6.1 (B). The boxed region in each merged panel is magnified on the right (bar, 2 µm). Bars, 5 µm (except for the magnified panel). A representative example is shown (n=3). (**C**) DIC or fluorescence microscopic image of wild-type, *rab-6.1* (RNAi), *rab-6.1 (tm2124)*, *rab-6.2* (RNAi), and *rab-6.2 (tm1924)* embryos in hypo- or hypertonic solutions (50 or 250 mM KCl, respectively) or FM4-64 solution. *rab-6.1*-depleted embryos were swollen in 50 mM KCl solution and shrunk in 250 mM KCl solution, and they were found to be permeable to FM4-64, indicating that they are osmotically fragile. A representative example is shown ($n \geq 5$). Bars, 5 µm. (**D**) Time series images of control (untreated) and *rab-6.1* (RNAi) embryos expressing both GFP::PH and GFP::tubulin during cytokinesis in the uterus. A representative example is shown (n=7). Bar, 5 µm.

rab-6.1 knockdown induces osmotic sensitivity, permeability and cytokinesis defects in embryos

To investigate the role played by Rab6 during *C. elegans* embryogenesis, we knocked down *rab-6.1* and *rab-6.2* via RNA interference (RNAi) treatment. Previous studies reported that the co-depletion of *rab-6.1* and *rab-6.2* results in embryonic lethality (Audhya et al., 2007; Zhang et al., 2008). We first confirmed that our RNAi treatment selectively depleted the RAB-6.1 or RAB-6.2 protein from the embryo (supplementary material Fig. S3). We found that the osmotic sensitivity of *rab-6.1* (RNAi) embryos was high, but that of *rab-6.2* (RNAi) embryos was not (Fig. 1C). *rab-6.1* (RNAi) embryos, but not *rab-6.2* (RNAi) embryos, were permeable to the lipophilic dye FM4-64 (Fig. 1C). We found a similar phenotype in the *rab-6.1*-deletion mutant *rab-6.1 (tm2124)*, which lacks 64% of the *rab-6.1* coding region, but not in the *rab-6.2*-deletion mutant, *rab-6.2 (tm1924)*, which lacks 18% of the *rab-6.2* coding region (Fig. 1C). High osmotic

sensitivity and incorporation of the lipophilic dye is a characteristic of defective permeability barrier formation due to the failure of cortical granule exocytosis (Rappleye et al., 1999; Sato et al., 2008). The number of embryos produced by *rab-6.1 (tm2124)* worms was ~29% of those produced by wild-type worms, and about 97% of the embryos were unhatched (supplementary material Fig. S2). Further, we confirmed that the cleavage furrow was hardly invaginated in the *rab-6.1* (RNAi) embryos (Fig. 1D). This phenotype is also observed in permeability barrier-defective embryos (Olson et al., 2006). The results suggest that RAB-6.1 is involved in the remodeling of the embryo surface.

RAB-6.1 is required for incorporation of cortical granules into the plasma membrane

To further evaluate the involvement of RAB-6.1 in cortical granule exocytosis, we examined the effect of *rab-6.1* RNAi on the dynamics of a cortical granule marker, a *C. elegans* caveolin-1 homolog CAV-1 (tagged with GFP; CAV-1::GFP) (Sato et al., 2006; Sato et al., 2008). In a previous study, all the 30 Rab GTPase genes were examined for their roles in cortical granule exocytosis, and the role of *rab-11.1* was reported (Sato et al., 2008) but that of *rab-6* was not. After the oocytes pass through the spermatheca, CAV-1 vesicles are tethered to the plasma membrane and incorporated into it (Fig. 2A; supplementary material Movie 1). We evaluated this incorporation process by using a transgenic strain expressing both CAV-1::GFP and the pleckstrin homology domain-containing membrane marker PH tagged with mCherry (mCherry::PH) (Kachur et al., 2008). Significant co-localization of CAV-1::GFP and mCherry::PH was observed when the cortical CAV-1 vesicles disappeared, indicating the incorporation of the CAV-1::GFP bodies into the plasma membrane (supplementary material Movie 1; Fig. 2A, middle column, 16 min). Later, during meiosis II, CAV-1 is re-internalized (supplementary material Movie 1; Fig. 2A, 24 min). In *rab-6.1* (RNAi) embryos, however, the CAV-1::GFP vesicles were not incorporated into the plasma membrane (supplementary material Movie 2; Fig. 2B, 16 and 24 min). An abnormal behavior of CAV-1::GFP vesicles was observed in *rab-6.1 (tm2124)* embryos, but not in *rab-6.2* (RNAi) or *rab-6.2 (tm1924)* embryos (supplementary material Fig. S4). These results indicate that RAB-6.1 is required for cortical granule exocytosis.

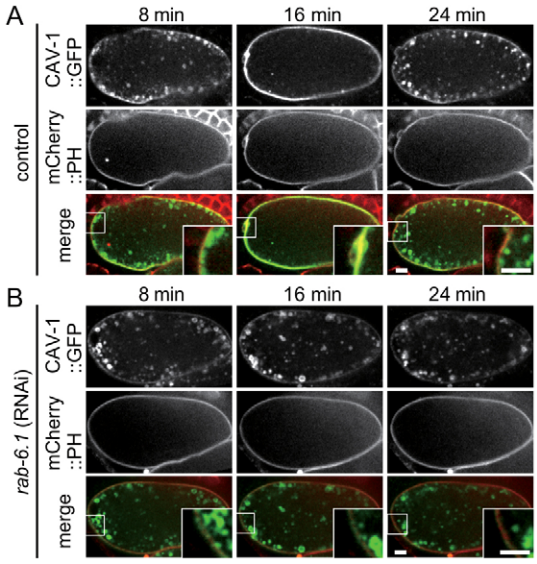

Fig. 2. RAB-6.1 is required for incorporation of cortical granules into the plasma membrane. Time series images of newly fertilized control (untreated) (**A**) and *rab-6.1* (RNAi) embryos (**B**) expressing both CAV-1::GFP and mCherry::PH. The boxed region in each merged panel is magnified on the right. The indicated times are determined from the exit of the oocyte from the spermatheca. In wild-type embryos, cortical granules are normally secreted about 15–16 min after the oocytes pass through the spermatheca. Bars, 5 μm.

Our observation suggested that RAB-6.2 plays a minor role in cortical granule exocytosis. We detected delayed and partial exocytosis of cortical granules (supplementary material Fig. S4) in the *rab-6.1*-deletion mutant embryos [*rab-6.1* (*tm2124*)], whereas the exocytosis was completely defective in *rab-6.1* (RNAi) (Fig. 2). We hypothesized that *rab-6.1* RNAi may slightly affect the expression of RAB-6.2, although we did not observe a detectable decrease in RAB-6.2 expression upon *rab-6.1* RNAi (supplementary material Fig. S3). We also hypothesized that simultaneous knockdown of RAB-6.1 and RAB-6.2 leads to a complete defect in cortical granule exocytosis. Consistent with this scenario, we observed a complete defect in cortical granule exocytosis after RAB-6.2 knockdown by RNAi in the *rab-6.1* (*tm2124*) strain (supplementary material Fig. S4). Of note is the finding that *rab-6.1* (*tm2124*); *rab-6.2* (*tm1924*) double deletion worms did not grow to adulthood, and we could not obtain embryos of this strain. These results indicate that RAB-6.2 can partially substitute the role of RAB-6.1 in cortical granule exocytosis. This role of RAB-6.2, however, is unlikely to be sufficient for functional exocytosis because *rab-6.1* (*tm2124*) alone showed a significant permeability barrier defect (Fig. 1C).

RAB-6.1 localizes to cortical granules

To investigate the role played by RAB-6.1 in cortical granule exocytosis, we analyzed its subcellular localization during cortical granule exocytosis. We generated a transgenic worm expressing both mCherry::RAB-6.1 and CAV-1::GFP and found that more than 90% of the mCherry::RAB-6.1 protein localized to the CAV-1::GFP vesicles in the oocytes (supplementary material Movie 3; Fig. 3A). Following fertilization, the RAB-6.1-positive CAV-1 vesicles are tethered to the plasma membrane. When the vesicles fused with the plasma membrane during meiotic anaphase I, the mCherry::RAB-6.1 signals from the CAV-1 bodies disappeared and were found dispersed throughout the cytoplasm (supplementary material Movie 4; Fig. 3B). This behavior is similar to that of Rab GTPase in vesicle trafficking after membrane fusion in other species (see Discussion). These results suggest that RAB-6.1 plays a role in membrane fusion between the cortical granules and plasma membrane.

To examine the role of GTP in RAB-6.1 localization, we expressed GDP-locked (T25N) and GTP-locked (Q70L) forms of RAB-6.1. While the GTP-locked form localized to the cortical granules, the GDP-locked form failed to do so (Fig. 3C). This result suggests that RAB-6.1 is in its GTP-bound form during the process. The expression of the GTP-locked form did not show an apparent dominant effect, suggesting that GTP-GDP exchange regulation of RAB-6.1 is relevant for the cortical granule localization of RAB-6.1 but not specifically for exocytosis.

The distribution of cortical granules in *rab-6.1* (RNAi) embryos is similar to that in embryos with defective cell cycle regulators

To obtain insights into the mechanisms of action of RAB-6.1, we compared the effect of *rab-6.1* inhibition on the intracellular distribution of cortical granules with the effects produced by the inhibition of other genes reported to be essential for cortical granule exocytosis (Bembenek et al., 2007; Sato et al., 2008). We performed RNAi for the membrane traffic regulator *rab-11.1* and the cell cycle regulators *emb-27 cdk-1*, and *sep-1* in CAV-1::GFP-expressing worms (supplementary material Movies 5–10; Fig. 4). *emb-27* and *cdk-1* encode the *C. elegans* orthologs of CDC16 (a subunit of APC/C) (Golden et al., 2000) and Cdk1 (Boxem et al., 1999), respectively. RAB-11.1 is involved in recruiting cortical granules to the plasma membrane (Sato et al., 2008). We confirmed that GFP::RAB-11.1 co-localizes with mCherry::RAB-6.1 vesicles near the plasma membrane until exocytosis (supplementary material Fig. S5). Consistent with the previous report (Sato et al., 2008), CAV-1 vesicles were strongly accumulated around the nucleus in the *rab-11.1* (RNAi) oocytes (supplementary material Movie 7; Fig. 4A). After fertilization, the CAV-1 vesicles were not tethered to the plasma membrane but were distributed throughout the cytoplasm in *rab-11.1* (RNAi) embryos (Fig. 4B). In contrast, *rab-6.1* (RNAi) embryos showed a different phenotype. After fertilization, the vesicles did not accumulated around the nucleus of the embryo; they are located near the plasma membrane but were not secreted (Fig. 4B). Of note, this phenotype was similar to that of the *cdk-1*, *emb-27* and *sep-1* (RNAi) embryos (Fig. 4B). On the basis of these results, we suspected that the role played by RAB-6.1 in cortical granule exocytosis is closely related to that of the cell cycle regulators downstream of the fertilization signal (CDK-1, EMB-27 and SEP-1).

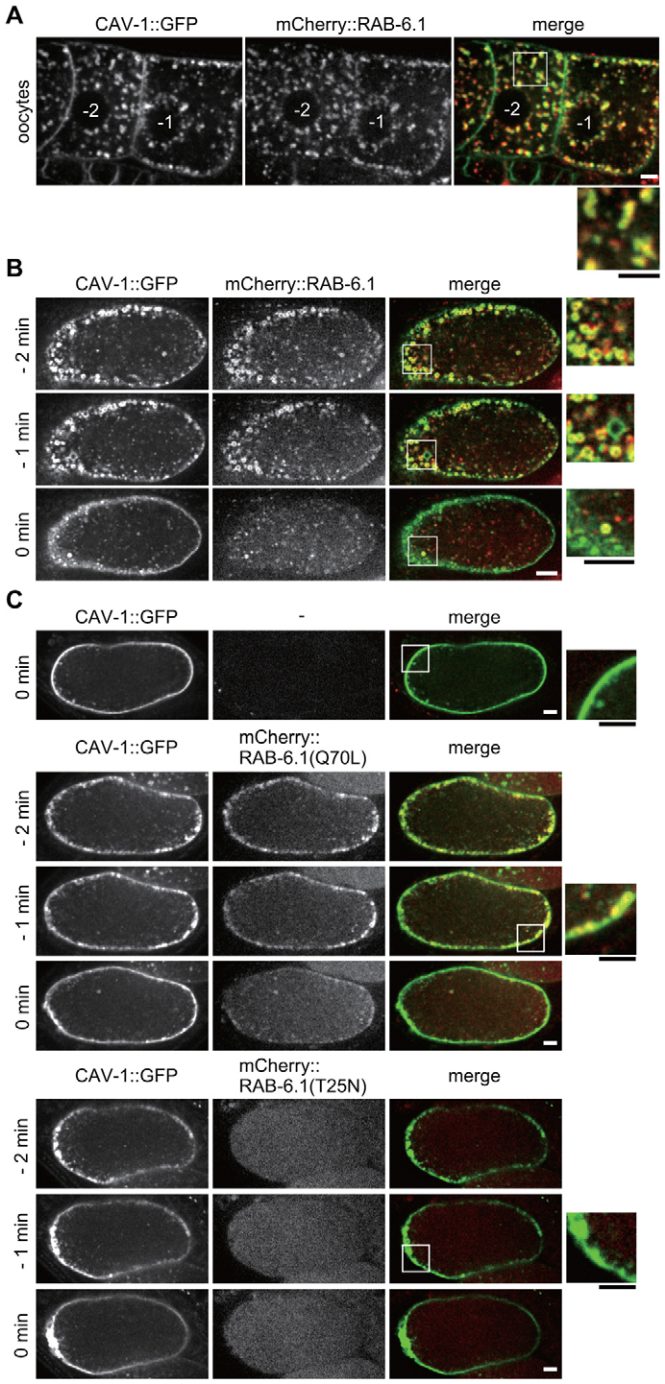

The recruitment of separase to cortical granules depends on RAB-6.1

Since the effects of RAB-6.1 inhibition on intracellular distribution of cortical granules were similar to those of CDK-1, EMB-27 and SEP-1 inhibition, we suspected a functional interaction between RAB-6.1 and cell cycle regulation. A previous study has revealed that SEP-1 localizes to the cortical granules during meiotic anaphase I and induced cortical granule exocytosis (Bembenek et al., 2007). SEP-1 has been also shown to be required for the fusion of secretory vesicles into the plasma membrane during cytokinesis (Bembenek et al., 2010). Thus, SEP-1 functions in membrane fusion, although the detailed mechanism is not known. We speculated that RAB-6.1 recruits SEP-1 to cortical granules to function as an effector protein during membrane fusion. We confirmed that GFP::SEP-1 translocates to RAB-6.1-positive cortical granules for 2 to 3 min before secretion (supplementary material Movie 11; Fig. 5A). The co-localization of SEP-1 and RAB-6.1 was observed even in *rab-11.1* (RNAi) embryos where RAB-6.1-positive cortical granules were not tethered to the plasma membrane (Fig. 5B; supplementary material Fig. S6). We examined the effect of *rab-6.1* RNAi on the recruitment of

Fig. 3. RAB-6.1 co-localizes with CAV-1. (**A**) Confocal fluorescence image of the most proximal oocyte ('−1') and the next most proximal oocyte ('−2') expressing CAV-1::GFP and mCherry::RAB-6.1. The boxed region in the merged panel is magnified below the panel. Bars, 5 µm. (**B**) Time series images of a newly fertilized embryo expressing both CAV-1::GFP and mCherry::RAB-6.1. The focal plane is set near the embryo surface in order to observe cortical granule exocytosis. The times are relative to the secretion of cortical granules. mCherry::RAB-6.1 co-localizes with CAV-1::GFP until just before granule secretion. The boxed region in each merged panel is magnified on the right. Bars, 5 µm. (**C**) Time series images of newly fertilized embryos expressing both CAV-1::GFP and the GTP-locked form [mCherry::RAB-6.1(Q70L)] or GDP-locked form of RAB-6.1 [mCherry::RAB-6.1(T25N)]. A control embryo expressing only CAV-1::GFP is also shown. The behavior of mCherry::RAB-6.1(Q70L) during cortical granule exocytosis was the same as that of wild-type RAB-6.1, whereas mCherry::RAB-6.1(T25N) failed to localize to the cortical granules. The boxed region in each merged panel is magnified on the right. The times are relative to the secretion of the cortical granules. Bars, 5 µm.

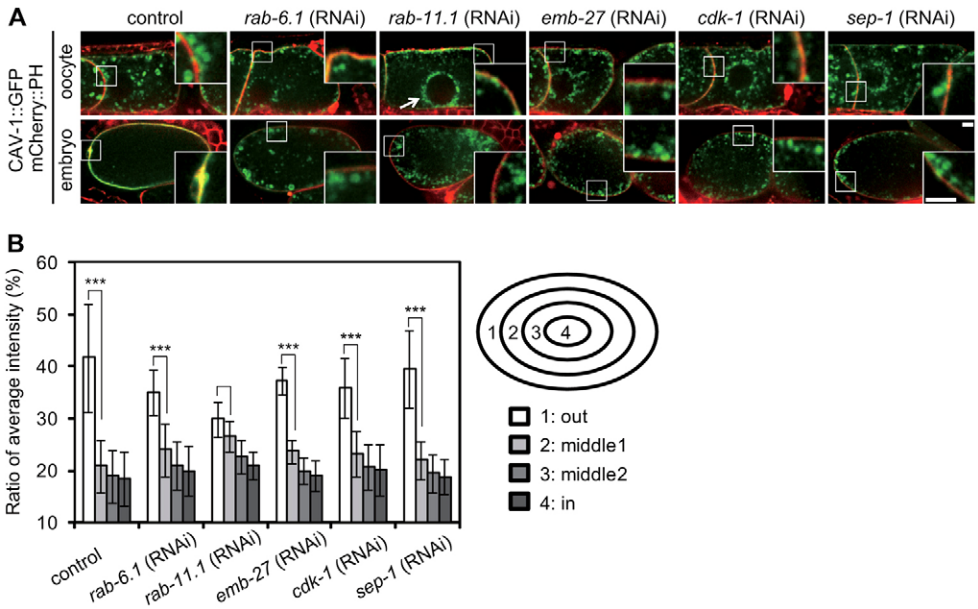

Fig. 4. Intracellular distribution of cortical granules. (**A**) Representative confocal fluorescence images of the most proximal oocytes (top) and newly fertilized embryos (bottom) expressing both CAV-1::GFP (green) and mCherry::PH (red) under the indicated RNAi conditions. The images of the central focal plane of the embryos are presented. The arrow in the image showing the *rab-11.1* (RNAi) oocyte indicates the abnormal accumulation of CAV-1::GFP around the nucleus. The images of fertilized embryos were taken 15–16 min after the oocytes passed through the spermatheca. Bars, 5 µm. (**B**) Average fluorescence intensity of CAV-1::GFP in the control ($n=7$), *rab-6.1* (RNAi) ($n=10$), *rab-11.1* (RNAi) ($n=8$), *emb-27* (RNAi) ($n=7$), *cdk-1* (RNAi) ($n=6$) and *sep-1* (RNAi) ($n=6$) embryos at 15–16 min after the oocytes passed through the spermatheca. The ratio of the average intensity across the four zones within an embryo is shown. Error bars: s.d. A schematic diagram of the four zones is shown on the right. A statistically significant difference between the outside area (‘1’) and the middle area (‘2’) is indicated by asterisks (***$P<0.005$). A statistically significant difference was also found between the outside area (‘1’) of the *rab-6.1* (RNAi) and *rab-11.1* (RNAi) embryos ($P=0.01$).

SEP-1 to the cortical granules and found that SEP-1 was not recruited in *rab-6.1* (RNAi) embryos (Fig. 5B). Chromosome separation did occur in *rab-6.1* (RNAi) embryos (Fig. 5B, arrows), indicating that the recruitment of SEP-1 to the cortical granules is independent of its chromosome segregation function. In contrast, polar body exclusion was defective in *rab-6.1* (RNAi) embryos, which is consistent with a previous report that proposed that extracellular space formation via cortical granule exocytosis is required for polar body exclusion (Bembenek et al., 2007).

SEP-1 recruitment to the cortical granules was not observed in *cdk-1* (RNAi) and *emb-27* (RNAi) embryos, in which chromosome separation and subsequent polar body extrusion did not occur (Fig. 5B). This result suggests that entry into anaphase is required for SEP-1 recruitment to the cortical granules. To induce the chromosome segregation function of separase, APC/C activates the protease activity of separase by degrading securin (Nasmyth, 2002). To recruit SEP-1 to the cortical granules, APC/C is required but the activation of SEP-1’s protease activity may not be required. The protease-dead form of SEP-1 (Bembenek et al., 2010) was still able to localize to the cortical granules (supplementary material Fig. S7). The role played by securin in SEP-1 localization to the cortical granules is not clear. Securin knockdown (*ify-1*) by RNAi did not induce ectopic recruitment of SEP-1 to the cortical granules but inhibited SEP-1 localization to the cortical granules and inhibited exocytosis (supplementary material Fig. S8). The stability of the SEP-1 protein may be reduced in *ify-1* (RNAi) *C. elegans* embryos, as reported in the case of human cells (Jallepalli et al., 2001).

The GTP- and GDP-bound forms of Rab GTPases are generally the active and inactive states, respectively, and the former can interact with effector proteins (Stenmark, 2009). Consistent with this general trend of Rab GTPases, we observed the co-localization of the GTP-locked (Q70L), but not GDP-locked (T25N), form of RAB-6.1 with SEP-1 (supplementary material Fig. S9A).

Consistent with the suggested minor role of RAB-6.2 in cortical granule exocytosis (supplementary material Fig. S4), RAB-6.2 likely plays a minor role also in SEP-1 localization to the cortical granules. We detected some SEP-1 positive cortical granules in the *rab-6.1*-deletion mutant embryos [*rab-6.1* (*tm2124*)], which were not detected after RAB-6.2 knockdown by RNAi in the *rab-6.1* (*tm2124*) strain (supplementary material Fig. S9B).

RAB-6.1 remains localized in unsecreted cortical granules in *sep-1* (RNAi) embryos

We observed that in normal embryos, RAB-6.1 temporarily co-localized with SEP-1 in the cortical granules for a few minutes and then was dispersed in the cytoplasm concomitantly with membrane fusion (Fig. 5A). Interestingly, in *sep-1* (RNAi) or *cdk-1* (RNAi) embryos, mCherry::RAB-6.1 did not dissociate from the cortical granules (supplementary material Movie 12; Fig. 5C). The result indicates that not only cortical granule exocytosis but also the dissociation of RAB-6.1 from the cortical granules depends on SEP-1. This further raises the possibility that the exocytosis triggers RAB-6.1 dissociation or vice versa and that the upstream event is triggered by SEP-1 (see Discussion).

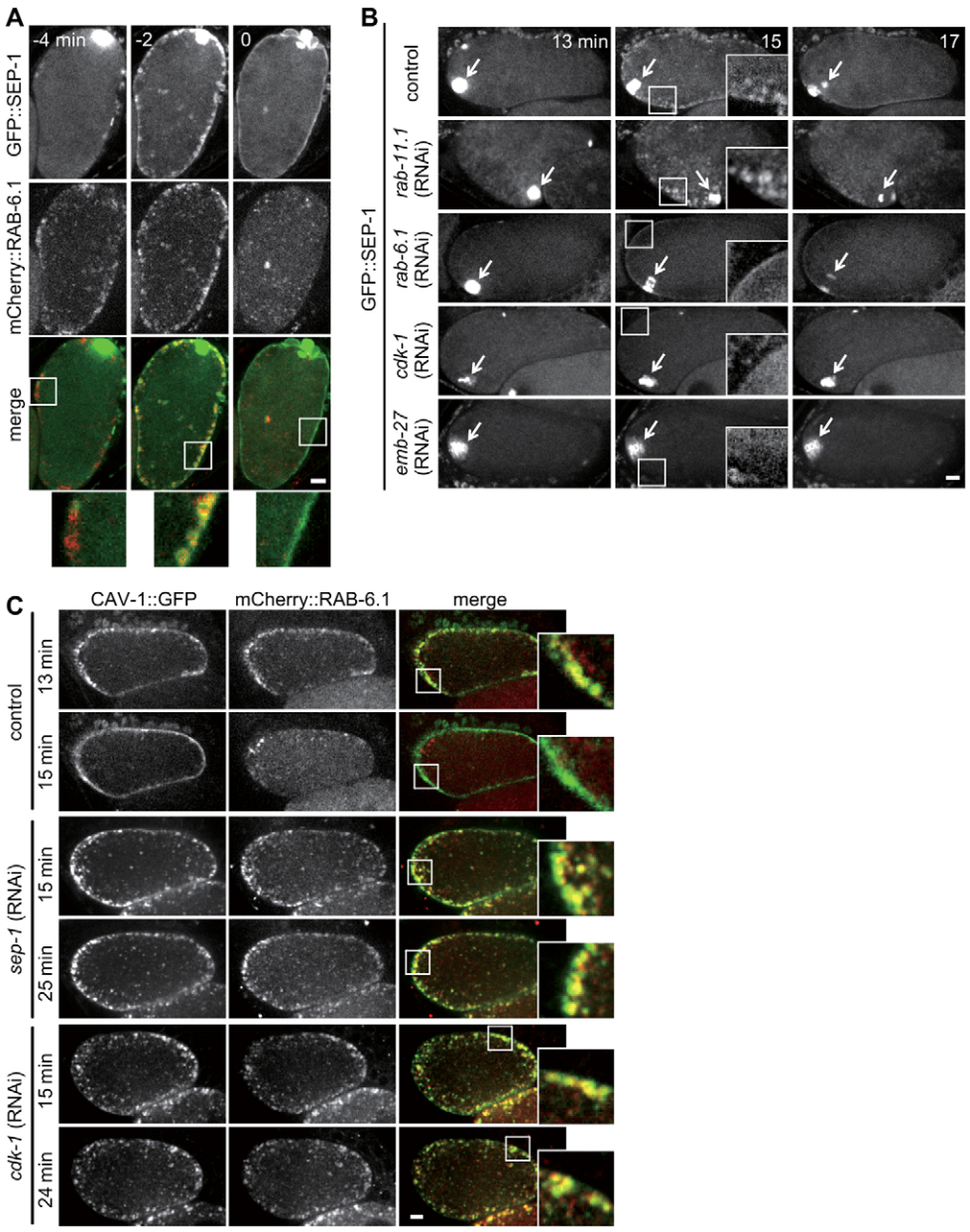

Fig. 5. SEP-1 recruitment to cortical granules depends on RAB-6.1. (**A**) Time series images of an embryo expressing both GFP::SEP-1 and mCherry::RAB-6.1. GFP::SEP-1 translocates to the cortical granules before they are secreted (−2 min). The boxed region in each merged panel is magnified on the bottom. The times are relative to cortical granule secretion. Bar, 5 µm. (**B**) Time series images of control, *rab-6.1* (RNAi), *rab-11.1* (RNAi), *emb-27* (RNAi), and *cdk-1* (RNAi) embryos expressing GFP::SEP-1. The boxed region in the middle panel is magnified on the right. GFP::SEP-1 translocation to the cortical granules was not observed in the *rab-6.1* (RNAi), *cdk-1* (RNAi), and *emb-27* (RNAi) embryos. Arrows indicate meiotic chromosomes of the oocyte. The indicated times are determined from the exit of the oocyte from the spermatheca. Bar, 5 µm. (**C**) Time series of control (top), *sep-1* (RNAi) (middle), and *cdk-1* (RNAi) (bottom) embryos expressing both CAV-1::GFP and mCherry::RAB-6.1. The indicated times are determined from the exit of the oocyte from the spermatheca. The boxed region in each merged panel is magnified on the right. Bar, 5 µm.

Discussion

We showed for the first time, to the best of our knowledge, that a *C. elegans* homolog of RAB6 GTPase, RAB-6.1, is required for cortical granules exocytosis during the oocyte-to-embryo transition (Fig. 6). Previous studies have shown that in addition to membrane traffic regulators, some cell cycle regulators are also involved in cortical granule exocytosis, so a link between cell cycle regulation and cortical granule exocytosis has been suggested (Sato et al., 2006; Bembenek et al., 2007). Because SEP-1 is required for the exocytosis of cortical granules (Bard et al., 2006; Bembenek et al., 2007; Bembenek et al., 2010), the timing of cortical granule secretion is considered to depend on

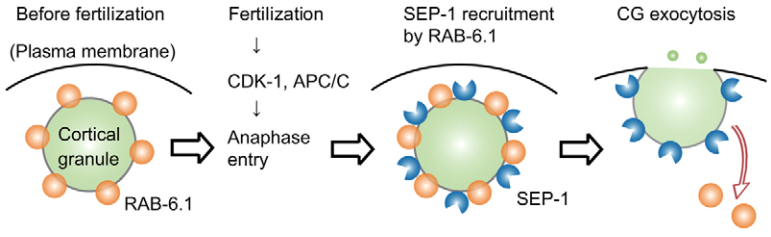

Fig. 6. A model for cortical granule exocytosis. Once the fertilization signal is received, the cell cycle progresses into meiotic anaphase I in a CDK-1- and APC/C-dependent manner. RAB-6.1 recruits SEP-1 to the cortical granules to promote their secretion. Concomitantly with membrane fusion, RAB-6.1 dissociates from the cortical granules.

SEP-1 under the control of cell cycle progression. It has been postulated that the recruitment of SEP-1 to cortical granules is required for cortical granule exocytosis, but how SEP-1 is recruited is not known. Moreover, previous studies found that the only way to prevent SEP-1 localization to cortical granules was to mutate SEP-1 itself. Therefore, the importance of the SEP-1 localization to the cortical granules was not clear. In this study, we found that the recruitment of SEP-1 to the cortical granules depends on RAB-6.1. Because both cortical granule exocytosis and SEP-1 recruitment to cortical granules were defective on *rab-6.1* knockdown, the hypothesis purporting the importance of SEP-1 localization to the cortical granules was supported. Our data indicate that RAB-6.1 is an important molecule that recruits separase after fertilization in meiotic anaphase I to the cortical granules to ensure timely exocytosis.

We were able to demonstrate that RAB-6.1 is essential for recruiting SEP-1 to the cortical granules, but the underlying molecular mechanism remains unclear. Because RAB-6.1 and SEP-1 co-localize on cortical granules, these 2 proteins may interact directly or indirectly. Generally, Rab GTPases interact with various effector proteins to recruit them to vesicles (Stenmark, 2009). Separase directly interacts with its regulators, securin and cyclin B (Gorr et al., 2005). We were not able to detect an interaction between RAB-6.1 and SEP-1 in a biochemical assay. Because the co-localization of RAB-6.1 and SEP-1 is observed in a very short period of time after fertilization (Fig. 5) even when RAB-6.1 is locked to its GTP form [RAB-6.1 (Q70L)] (supplementary material Fig. S9A), it may be difficult to demonstrate the biochemical interaction between the RAB-6.1 and SEP-1 proteins.

Our experiments using the GTP- and GDP-locked forms of RAB-6.1 indicated that RAB-6.1 should be in its GTP-bound form to be localized to the cortical granules (Fig. 3C). In humans, Rab6 is phosphorylated via a protein kinase C-dependent mechanism in activated platelets, and phosphorylated Rab6 has a higher affinity for GTP than GDP *in vitro* (Fitzgerald and Reed, 1999). The consensus phosphorylation site is conserved in *C. elegans* (Fitzgerald and Reed, 1999). However, no experimental support is currently available for the hypothesis that RAB-6.1 must be phosphorylated for its localization to the cortical granules. Interestingly, however, the depletion of protein phosphatase 5 (PPH-5) suppresses the localization defect for two of the three *sep-1* alleles that have a specific defect in SEP-1 localization to the cortical granules (Bembenek et al., 2007; Richie et al., 2011). It has been proposed that phosphorylation is involved in the regulation of SEP-1 localization, and that SEP-1 is a plausible target of the phosphorylation (Richie et al., 2011). Alternatively, RAB-6.1 may be a target for phosphoregulation, and PPH-5 depletion may lead to increased levels of the GTP-bound form of RAB-6.1 and of the RAB-6.1 protein on cortical granules in order to suppress some of the *sep-1* alleles.

The behavior of RAB-6.1 during cortical granule exocytosis would be a useful model to study the spatiotemporal regulation of Rab GTPases. We showed the dynamic behavior of a Rab GTPase, in that RAB-6.1 temporarily co-localized with SEP-1 on cortical granules for a few minutes and then was dispersed in the cytoplasm concomitantly with membrane fusion (Fig. 5A). We initially suspected that this dynamic change in the subcellular localization of RAB-6.1 might reflect conversion between GDP- and GTP-bound forms (Pfeffer and Aivazian, 2004; Stenmark, 2009). In general, guanine nucleotide exchange factors (GEFs) and GTPase-activating proteins (GAPs) switch between these two states (Stenmark, 2009; Barr and Lambright, 2010). However, we observed the normal dynamic behavior of the GTP-locked form of RAB-6.1 (Fig. 3C; supplementary material Fig. S9A), and thus, the spatiotemporal regulation of RAB-6.1 during cortical granule exocytosis may not involve GTP-GDP exchange. We found that in *sep-1* (RNAi) embryos, the cortical granules did not fuse with the plasma membrane, and RAB-6.1 remained on the unsecreted cortical granules (Fig. 5C). Thus, a possible regulatory mechanism could be that SEP-1 induces cortical granule exocytosis, and the exocytosis triggers the dissociation of RAB-6.1 from the granules. Alternatively, SEP-1 may trigger the dissociation of RAB-6.1, which may in turn trigger membrane fusion. Further characterization of the relationship between SEP-1 and RAB-6.1 should provide a clue for understanding the spatiotemporal regulation of Rab GTPases and its consequences.

Materials and Methods

Strains and manipulation of *C. elegans*

C. elegans strains were maintained using standard techniques (Brenner, 1974). The strains used in this study are listed in supplementary material Table S1. For construction of the CAL0384 and CAL0396 strains, the full-length DNA of *rab-6.1* or *rab-6.2* was amplified using polymerase chain reaction (PCR) from *C. elegans* genomic DNA. For construction of the CAL0621 and CAL0641 strains, the full-length *rab-6.1* DNA was engineered to be in the GTP-locked (Q70L) or GDP-locked (T25N) forms by site-directed mutagenesis. The full-length gene was cloned into the *pie-1*-based vector pID3.01B or mCherry_N_GW vector. The latter was obtained by modifying the *pie-1*-based vector TH312-Cherry(n) (R. Arai, unpublished). The promoter and 3′ UTR regulatory sequences used to drive *rab-6.1* and *rab-6.2* expression were derived from *pie-1*. The pID3.01B and TH312-Cherry(n) vectors were provided by G. Seydoux and A. Hyman, respectively. Transgenic worms were created using the microparticle bombardment technique (Praitis et al., 2001). The *rab-6.1 (tm2124)* and *rab-6.2 (tm1924)* mutants were obtained from National Bioresource Project for the Experimental Animal 'Nematode *C. elegans*', and backcrossed to wild-type N2 four and five times, respectively. For *rab-6.1* (*tm2124*), the first 556 bp including the start codon and upstream 348 bp was deleted. For *rab-6.2* (*tm1924*), a 774-bp internal region was deleted, so it would generate a truncated protein. This truncated RAB-6.2 lacks one of the conserved GTP-binding domains and thus is probably not functional. The deletion mutation in the mutants analyzed in this study was confirmed using the single worm PCR method (Williams et al., 1992) with slight modifications and the following primer sets: 5′-TGGCTGATTTCACAAATAACGCT-3′ and 5′-AACACGGACATTGACGGCCT-3′ (Rual et al., 2004) for *rab-6.1 (tm2124)* and 5′-AGCGCTTTTAAGGGGGATAA-3′ and 5′-TGTACTTGGAGGACCGAACC-3′ (Sönnichsen et al., 2005) for *rab-6.2 (tm1924)*. The *rab-6.1 (tm2124)* mutation was maintained by creating a balancer strain by crossing with HS732 (*wrm-1(tm514)* III/*hT2*[*bli-4(e937) let-?(q782) qIs48*] (I;III)). CAL0011, CAL0421, CAL0431, CAL0501, CAL0511, CAL0531, CAL0671, CAL0681, CAL0731, CAL0741, CAL0652, CAL0691, CAL0721, CAL0701, CAL0751, and CAL0711 were obtained by crossing AZ244 with OD58, RT688 with OD70, RT688 with CAL0396, WH347 with CAL0396, WH416 with CAL0396, CAL0384 with CAL0396, WH416 with CAL0621, RT688 with CAL0621, WH416 with CAL0641, RT688 with CAL0641, *rab-6.1 (tm2124)* with HS732, CAL0652 with RT688, CAL0652 with WH416, CAL0652 with CAL0396, *rab-6.2 (tm1924)* with RT688, and *rab-6.2 (tm1924)* with WH416, respectively.

RNA interference

RNAi was performed by injecting double-stranded RNAs (dsRNAs) as described previously (Hara and Kimura, 2009). The dsRNAs were amplified using PCR from *C. elegans* genomic DNA. The primer sets used for amplification of dsRNAs in this study are the same as those in PhenoBank (http://www.worm.mpi-cbg.de/phenobank2/cgi-bin/MenuPage.py) except in the case of *rab-6.1*. For *rab-6.1*, the following primers were used: 5′-TAATACGACTCACTATAGGCAGACAAGTTTCGACGGAGGATG-3′ and 5′-AATTAACCCTCACTAAAGGTTGACGGCCTTGGCTCTCT-3′. Worms injected with dsRNA were incubated at 22℃ for 22–30 h before analysis of oocytes and embryos.

Microscopy

For microscopic analysis, the worms were placed in a drop of M9 buffer containing 1 mM levamisole on an agar pad (2%) and covered with a coverslip. For FM4-64 staining, embryos were dissected from gravid hermaphrodites in 150 mM KCl

containing 5 mM HEPES (pH 7.2) and 33 μM FM4-64 (Molecular Probes, Carlsbad, CA) and incubated for 10 minutes at room temperature in the dark. Fluorescence images were visualized using a spinning-disk confocal system (CSU-X1; Yokogawa, Tokyo, Japan) mounted on a microscope (BX71; Olympus, Tokyo, Japan) equipped with a UPlanSApo 60×1.30 NA or 100×1.40 NA objective (Olympus) at room temperature. Digital images were obtained using a charge-coupled device (CCD) camera (iXon; Andor, Belfast, UK) controlled by the Metamorph software (Molecular Devices, Downington, PA). For analysis of osmotic sensitivity, embryos were dissected from gravid hermaphrodites in hypotonic or hypertonic solutions (50 or 250 mM KCl, respectively). To prevent compression by a coverslip, the embryos were placed in a drop of the solution in the wells of a slide glass (Multitest slide 8-well; MP Biomedicals LLC, Solon, OH) and covered with a coverslip. To obtain differential interference contrast (DIC) images of the embryos under each condition, the embryos were viewed under a microscope (BX51; Olympus) equipped with a UPlanSApo 60×1.20 NA objective at room temperature. Digital images were obtained with a CCD camera (ORCA-ER; Hamamatsu, Japan) controlled by the IPLab software (BD Biosciences, Rockville, MD).

Quantification of the intracellular distribution of cortical granules

To quantify the intracellular distribution of cortical granules, the average fluorescence intensity of CAV-1::GFP-expressing embryos was measured just before granule secretion (15–16 min after fertilization) (Fig. 4B) by using the IPLab software. The area of each embryo in the confocal section was divided into 4 zones from the outside: we first drew an oval along the edges of the embryos by judging visually. Then, we drew ovals that were 3/4, 1/2 and 1/4 the size of the original oval by using the software (Fig. 4B). The average fluorescence intensity was normalized by subtracting the average intensity of a background region.

Statistical analysis

The statistical difference in the ratio of the average intensity of CAV-1::GFP between the outside area (‘1’) and the middle area (‘2’) in each condition (Fig. 4B) was determined using the two-tailed paired Student’s *t*-test. The normality of the data was assessed by using the Shapiro-Wilk test. P values <0.05 were considered statistically significant.

Acknowledgements

We are grateful to Drs K. Sato (Gunma University, Japan) and S. Ihara (National Institute of Genetics, Mishima, Japan) for technical advice, J. Ahringer (University of Cambridge, Cambridge, UK), A. Hyman (Max Planck Institute of Molecular Cell Biology and Genetics, Germany), H. Sawa and Y. Kohara (National Institute of Genetics, Mishima, Japan), G. Seydoux (Johns Hopkins University, USA), J. N. Bembenek (University of Michigan, USA) and National Bioresource Project (S. Mitani Laboratory, Tokyo Women’s Medical University, Japan) for providing strains. Strains were also provided by the *Caenorhabditis* Genetics Center, funded by the National Institutes of Health. We thank Dr R. Arai (National Institute of Genetics) for sharing unpublished material, and the members of our laboratory for critical reading of the manuscript.

Funding

This study was supported by a KAKENHI (Grant in Aid for Scientific Research) and by the Transdisciplinary Research Integration Center of the Research Organization of Information and Systems, Japan.

Supplementary material available online at
http://jcs.biologists.org/lookup/suppl/doi:10.1242/jcs.116400/-/DC1

References

Andrews, R. and Ahringer, J. (2007). Asymmetry of early endosome distribution in *C. elegans* embryos. *PLoS ONE* **2**, e493.

Audhya, A., Hyndman, F., McLeod, I. X., Maddox, A. S., Yates, J. R., 3rd, Desai, A. and Oegema, K. (2005). A complex containing the Sm protein CAR-1 and the RNA helicase CGH-1 is required for embryonic cytokinesis in *Caenorhabditis elegans*. *J. Cell Biol.* **171**, 267-279.

Audhya, A., Desai, A. and Oegema, K. (2007). A role for Rab5 in structuring the endoplasmic reticulum. *J. Cell Biol.* **178**, 43-56.

Bard, F., Casano, L., Mallabiabarrena, A., Wallace, E., Saito, K., Kitayama, H., Guizzunti, G., Hu, Y., Wendler, F., Dasgupta, R. et al. (2006). Functional genomics reveals genes involved in protein secretion and Golgi organization. *Nature* **439**, 604-607.

Barr, F. and Lambright, D. G. (2010). Rab GEFs and GAPs. *Curr. Opin. Cell Biol.* **22**, 461-470.

Bembenek, J. N., Richie, C. T., Squirrell, J. M., Campbell, J. M., Eliceiri, K. W., Poteryaev, D., Spang, A., Golden, A. and White, J. G. (2007). Cortical granule exocytosis in *C. elegans* is regulated by cell cycle components including separase. *Development* **134**, 3837-3848.

Bembenek, J. N., White, J. G. and Zheng, Y. (2010). A role for separase in the regulation of RAB-11-positive vesicles at the cleavage furrow and midbody. *Curr. Biol.* **20**, 259-264.

Boxem, M., Srinivasan, D. G. and van den Heuvel, S. (1999). The *Caenorhabditis elegans* gene *ncc-1* encodes a *cdc2*-related kinase required for M phase in meiotic and mitotic cell divisions, but not for S phase. *Development* **126**, 2227-2239.

Brenner, S. (1974). The genetics of *Caenorhabditis elegans*. *Genetics* **77**, 71-94.

Conner, S. D. and Wessel, G. M. (2001). Syntaxin, VAMP, and Rab3 are selectively expressed during sea urchin embryogenesis. *Mol. Reprod. Dev.* **58**, 22-29.

Conner, S., Leaf, D. and Wessel, G. (1997). Members of the SNARE hypothesis are associated with cortical granule exocytosis in the sea urchin egg. *Mol. Reprod. Dev.* **48**, 106-118.

Echard, A., Jollivet, F., Martinez, O., Lacapère, J. J., Rousselet, A., Janoueix-Lerosey, I. and Goud, B. (1998). Interaction of a Golgi-associated kinesin-like protein with Rab6. *Science* **279**, 580-585.

Ferrell, J. E., Jr (1999). *Xenopus* oocyte maturation: new lessons from a good egg. *Bioessays* **21**, 833-842.

Fitzgerald, M. L. and Reed, G. L. (1999). Rab6 is phosphorylated in thrombin-activated platelets by a protein kinase C-dependent mechanism: effects on GTP/GDP binding and cellular distribution. *Biochem. J.* **342**, 353-360.

Fukuda, Y. and Chang, M. C. (1978). The time of cortical granule breakdown and sperm penetration in mouse and hamster eggs inseminated in vitro. *Biol. Reprod.* **19**, 261-266.

Golden, A., Sadler, P. L., Wallenfang, M. R., Schumacher, J. M., Hamill, D. R., Bates, G., Bowerman, B., Seydoux, G. and Shakes, D. C. (2000). Metaphase to anaphase (*mat*) transition-defective mutants in *Caenorhabditis elegans*. *J. Cell Biol.* **151**, 1469-1482.

Gorr, I. H., Boos, D. and Stemmann, O. (2005). Mutual inhibition of separase and Cdk1 by two-step complex formation. *Mol. Cell* **19**, 135-141.

Grigoriev, I., Splinter, D., Keijzer, N., Wulf, P. S., Demmers, J., Ohtsuka, T., Modesti, M., Maly, I. V., Grosveld, F., Hoogenraad, C. C. et al. (2007). Rab6 regulates transport and targeting of exocytotic carriers. *Dev. Cell* **13**, 305-314.

Grigoriev, I., Yu, K. L., Martinez-Sanchez, E., Serra-Marques, A., Smal, I., Meijering, E., Demmers, J., Peränen, J., Pasterkamp, R. J., van der Sluijs, P. et al. (2011). Rab6, Rab8, and MICAL3 cooperate in controlling docking and fusion of exocytotic carriers. *Curr. Biol.* **21**, 967-974.

Hara, Y. and Kimura, A. (2009). Cell-size-dependent spindle elongation in the *Caenorhabditis elegans* early embryo. *Curr. Biol.* **19**, 1549-1554.

Horner, V. L. and Wolfner, M. F. (2008). Transitioning from egg to embryo: triggers and mechanisms of egg activation. *Dev. Dyn.* **237**, 527-544.

Jallepalli, P. V., Waizenegger, I. C., Bunz, F., Langer, S., Speicher, M. R., Peters, J. M., Kinzler, K. W., Vogelstein, B. and Lengauer, C. (2001). Securin is required for chromosomal stability in human cells. *Cell* **105**, 445-457.

Januschke, J., Nicolas, E., Compagnon, J., Formstecher, E., Goud, B. and Guichet, A. (2007). Rab6 and the secretory pathway affect oocyte polarity in *Drosophila*. *Development* **134**, 3419-3425.

Kachur, T. M., Audhya, A. and Pilgrim, D. B. (2008). UNC-45 is required for NMY-2 contractile function in early embryonic polarity establishment and germline cellularization in *C. elegans*. *Dev. Biol.* **314**, 287-299.

Kline, D. and Kline, J. T. (1992). Repetitive calcium transients and the role of calcium in exocytosis and cell cycle activation in the mouse egg. *Dev. Biol.* **149**, 80-89.

Kosinski, M., McDonald, K., Schwartz, J., Yamamoto, I. and Greenstein, D. (2005). *C. elegans* sperm bud vesicles to deliver a meiotic maturation signal to distant oocytes. *Development* **132**, 3357-3369.

Lawrence, Y., Whitaker, M. and Swann, K. (1997). Sperm-egg fusion is the prelude to the initial Ca^{2+} increase at fertilization in the mouse. *Development* **124**, 233-241.

Leguia, M., Conner, S., Berg, L. and Wessel, G. M. (2006). Synaptotagmin I is involved in the regulation of cortical granule exocytosis in the sea urchin. *Mol. Reprod. Dev.* **73**, 895-905.

Marcello, M. R. and Singson, A. (2010). Fertilization and the oocyte-to-embryo transition in C. elegans. *BMB Rep.* **43**, 389-399.

Matanis, T., Akhmanova, A., Wulf, P., Del Nery, E., Weide, T., Stepanova, T., Galjart, N., Grosveld, F., Goud, B., De Zeeuw, C. I. et al. (2002). Bicaudal-D regulates COPI-independent Golgi-ER transport by recruiting the dynein-dynactin motor complex. *Nat. Cell Biol.* **4**, 986-992.

Matson, S., Markoulaki, S. and Ducibella, T. (2006). Antagonists of myosin light chain kinase and of myosin II inhibit specific events of egg activation in fertilized mouse eggs. *Biol. Reprod.* **74**, 169-176.

McCarter, J., Bartlett, B., Dang, T. and Schedl, T. (1999). On the control of oocyte meiotic maturation and ovulation in *Caenorhabditis elegans*. *Dev. Biol.* **205**, 111-128.

Miserey-Lenkei, S., Chalancon, G., Bardin, S., Formstecher, E., Goud, B. and Echard, A. (2010). Rab and actomyosin-dependent fission of transport vesicles at the Golgi complex. *Nat. Cell Biol.* **12**, 645-654.

Mizuguchi, S., Uyama, T., Kitagawa, H., Nomura, K. H., Dejima, K., Gengyo-Ando, K., Mitani, S., Sugahara, K. and Nomura, K. (2003). Chondroitin proteoglycans are involved in cell division of *Caenorhabditis elegans*. *Nature* **423**, 443-448.

Nasmyth, K. (2002). Segregating sister genomes: the molecular biology of chromosome separation. *Science* **297**, 559-565.

Olson, S. K., Bishop, J. R., Yates, J. R., Oegema, K. and Esko, J. D. (2006). Identification of novel chondroitin proteoglycans in *Caenorhabditis elegans*: embryonic cell division depends on CPG-1 and CPG-2. *J. Cell Biol.* **173**, 985-994.

Pellettieri, J., Reinke, V., Kim, S. K. and Seydoux, G. (2003). Coordinate activation of maternal protein degradation during the egg-to-embryo transition in *C. elegans*. *Dev. Cell* **5**, 451-462.

Pfeffer, S. and Aivazian, D. (2004). Targeting Rab GTPases to distinct membrane compartments. *Nat. Rev. Mol. Cell Biol.* **5**, 886-896.

Praitis, V., Casey, E., Collar, D. and Austin, J. (2001). Creation of low-copy integrated transgenic lines in *Caenorhabditis elegans*. *Genetics* **157**, 1217-1226.

Rappleye, C. A., Paredez, A. R., Smith, C. W., McDonald, K. L. and Aroian, R. V. (1999). The coronin-like protein POD-1 is required for anterior-posterior axis formation and cellular architecture in the nematode *Caenorhabditis elegans*. *Genes Dev.* **13**, 2838-2851.

Richie, C. T., Bembenek, J. N., Chestnut, B., Furuta, T., Schumacher, J. M., Wallenfang, M. and Golden, A. (2011). Protein phosphatase 5 is a negative regulator of separase function during cortical granule exocytosis in *C. elegans*. *J. Cell Sci.* **124**, 2903-2913.

Rual, J. F., Ceron, J., Koreth, J., Hao, T., Nicot, A. S., Hirozane-Kishikawa, T., Vandenhaute, J., Orkin, S. H., Hill, D. E., van den Heuvel, S. et al. (2004). Toward improving *Caenorhabditis elegans* phenome mapping with an ORFeome-based RNAi library. *Genome Res.* **14**, 2162-2168.

Runft, L. L., Jaffe, L. A. and Mehlmann, L. M. (2002). Egg activation at fertilization: where it all begins. *Dev. Biol.* **245**, 237-254.

Samuel, A. D., Murthy, V. N. and Hengartner, M. O. (2001). Calcium dynamics during fertilization in *C. elegans*. *BMC Dev. Biol.* **1**, 8.

Sato, K., Sato, M., Audhya, A., Oegema, K., Schweinsberg, P. and Grant, B. D. (2006). Dynamic regulation of caveolin-1 trafficking in the germ line and embryo of *Caenorhabditis elegans*. *Mol. Biol. Cell* **17**, 3085-3094.

Sato, M., Grant, B. D., Harada, A. and Sato, K. (2008). Rab11 is required for synchronous secretion of chondroitin proteoglycans after fertilization in *Caenorhabditis elegans*. *J. Cell Sci.* **121**, 3177-3186.

Siomos, M. F., Badrinath, A., Pasierbek, P., Livingstone, D., White, J., Glotzer, M. and Nasmyth, K. (2001). Separase is required for chromosome segregation during meiosis I in *Caenorhabditis elegans*. *Curr. Biol.* **11**, 1825-1835.

Sönnichsen, B., Koski, L. B., Walsh, A., Marschall, P., Neumann, B., Brehm, M., Alleaume, A. M., Artelt, J., Bettencourt, P., Cassin, E. et al. (2005). Full-genome RNAi profiling of early embryogenesis in *Caenorhabditis elegans*. *Nature* **434**, 462-469.

Stenmark, H. (2009). Rab GTPases as coordinators of vesicle traffic. *Nat. Rev. Mol. Cell Biol.* **10**, 513-525.

Wessel, G. M., Brooks, J. M., Green, E., Haley, S., Voronina, E., Wong, J., Zaydfudim, V. and Conner, S. (2001). The biology of cortical granules. *Int. Rev. Cytol.* **209**, 117-206.

Williams, B. D., Schrank, B., Huynh, C., Shownkeen, R. and Waterston, R. H. (1992). A genetic mapping system in *Caenorhabditis elegans* based on polymorphic sequence-tagged sites. *Genetics* **131**, 609-624.

Zhang, H., Squirrell, J. M. and White, J. G. (2008). RAB-11 permissively regulates spindle alignment by modulating metaphase microtubule dynamics in *Caenorhabditis elegans* early embryos. *Mol. Biol. Cell* **19**, 2553-2565.